红外与激光工程
INFRARED AND LASER ENGINEERING
EI, SCOPUS, CSCD等收录期刊

Yb,Ho,Pr:GYTO晶体生长、结构及光谱性能（特邀）

何 窦仁勤 张昊天 刘文鹏 张庆礼 陈迎迎 高宇茜 罗建乔

Growth, structure, and spectroscopic properties of Yb,Ho,Pr:GYTO single crystal *Invited*

He Yi, Dou Renqin, Zhang Haotian, Liu Wenpeng, Zhang Qingli, Chen Yingying, Gao Yuxi, Luo Jianqiao

在线阅读 View online: https://doi.org/10.3788/IRLA20201067

Growth, structure, and spectroscopic properties of Yb,Ho,Pr:GYTO single crystal (*Invited*)

He Yi[1,2], Dou Renqin[1*], Zhang Haotian[1,2], Liu Wenpeng[1], Zhang Qingli[1*], Chen Yingying[1,2], Gao Yuxi[1,2], Luo Jianqiao[1]

(1. The Key Laboratory of Photonic Devices and Materials, Anhui Province, Anhui Institute of Optics and Fine Mechanics, Hefei institutes of Physical Science, Chinese Academy of Sciences, Hefei 230031, PR China;
2. University of Science and Technology of China, Hefei 230026, PR China)

Abstract: A new mid infrared laser material Yb,Ho,Pr:GYTO crystal was grown successfully using Czochralski method for the first time. The structural parameters were obtained by the X-ray Rietveld refinement method. The X-ray rocking curves of the (100), (010), and (001) diffraction face of Yb,Ho,Pr:GYTO crystal were measured. The full widths at half maximum of those diffraction peaks are 0.036°, 0.013°, and 0.077°, respectively, which indicates a high crystalline quality of the as-grown crystal. Laser Ablation Inductively-Coupled Plasma Mass Spectrometry was used to measure the concentrations of Yb^{3+}, Ho^{3+}, Pr^{3+}, and Y^{3+} ions in the Yb,Ho,Pr:$GdYTaO_4$ crystal. The effective segregation coefficients of Yb^{3+}, Ho^{3+}, Pr^{3+}, and Y^{3+} in Yb,Ho,Pr:GYTO crystal are 0.624, 1.220, 1.350, and 0.977, respectively. The room-temperature polarhosized absorption spectra of Yb,Ho, Pr:$GdYTaO_4$ was measured and the corresponding absorption transitions were assigned. The 2.9 μm fluorescence spectrum excited by 940 nm LD presents that the strongest emission is located at 2908 nm. In addition, the Yb-Ho-Pr energy transfer mechanism in GYTO was also demonstrated. Compared with Ho:GYTO crystal, the lifetime of $^5I_7$ level of Yb,Ho,Pr:GYTO crystal is reduced by 87.13%, which is close to that of the upper level $^5I_6$, indicating that Yb,Ho,Pr:GYTO crystal is easier to realize population inversion and laser output.

Key words: Yb,Ho,Pr:GYTO; crystal growth; spectra; lifetime
CLC number: O782 **Document code:** A **DOI:** 10.3788/IRLA20201067

Yb,Ho,Pr:GYTO 晶体生长、结构及光谱性能 (特邀)

何 異[1,2], 窦仁勤[1*], 张昊天[1,2], 刘文鹏[1], 张庆礼[1*], 陈迎迎[1,2], 高宇茜[1,2], 罗建乔[1]

(1. 中国科学院合肥物质科学研究院安徽光学精密机械研究所 光子器件与材料安徽省重点实验室, 安徽 合肥 230031;
2. 中国科学技术大学, 安徽 合肥 230026)

摘 要: 首次采用提拉法成功生长出了新型中红外激光晶体 Yb,Ho,Pr:GYTO, 采用 X 射线 Rietveld 精修方法得到了晶体的结构参数。测量了 Yb,Ho,Pr:GYTO 晶体 (100)、(010) 和 (001) 衍射面的 X 射线

收稿日期: 2020−10−20; **修订日期:** 2020−11−25
基金项目: 国家自然科学基金青年基金 (51802307); 中国科学院合肥物质科学研究院院长基金 (YZJJ2018QN3); 国家重点研发计划 (2016YFB0402101); 中国科学院联合基金 (6141A01080302)
作者简介: 何異 (1993−), 女, 博士生, 主要从事晶体的生长和数值模拟研究。Email: hy614@mail.ustc.edu.cn
通讯作者: 窦仁勤 (1987−), 女, 博士, 主要从事光学功能晶体的生长和表征。Email: drq0564@aiofm.ac.cn
张庆礼 (1973−), 男, 研究员, 博士生导师, 主要从事光功能晶体材料研究。Email: zql@aiofm.ac.cn

摇摆曲线，衍射峰的半峰宽分别为 0.036°、0.013°和 0.077°，表明生长出的晶体是单晶并且具有较高的结晶质量。采用激光剥蚀电感耦合等离子体质谱法测定了 Yb,Ho,Pr:GYTO 晶体中 Yb^{3+}、Ho^{3+}、Pr^{3+}和 Y^{3+}的浓度，Yb,Ho,Pr:GYTO 晶体中 Yb^{3+}、Ho^{3+}、Pr^{3+}和 Y^{3+}的有效分凝系数分别为 0.624、1.220、1.350 和 0.977。测量了 Yb,Ho,Pr:GYTO 晶体室温下的极化吸收谱，并指认了相应的能级吸收跃迁。940 nm 半导体激光器激发的 2.9 μm 荧光光谱表明，最大发射波长为 2908 nm。此外，还论证了 GYTO 中 Yb-Ho-Pr 的能量传递机制。与 Ho:GYTO 晶体相比，Yb,Ho,Pr:GYTO 晶体的 $^5I_7$ 能级寿命降低了 87.13%，与上能级 $^5I_6$ 的寿命相近，说明 Yb,Ho,Pr:GYTO 晶体更容易实现粒子数反转和激光输出。

关键词： Yb,Ho,Pr:GYTO； 晶体生长； 光谱； 寿命

0 Introduction

Previously, rare-earth orthotantalate ($RETaO_4$) had been attracted as scintillator crystals and X-ray phosphors, due to its high chemical stability, high density, rich physical properties, and so on[1−2]. $RETaO_4$ belongs to the fergusonite structure and exhibits excellent luminescent properties[3−6]. It usually exhibits two modifications, fergusonite M-type structure I2/a (C_{2h}^6, #15, Z = 4), and fergusonite M'-type structure P2/a (C_{2h}^4, #13, Z = 2)[7]. RE ions, with similar ion radius, can be substituted easily by other rare earth ions to realize characteristic emission[8]. Besides, $RETaO_4$ belong to monoclinic system and the site of RE ions is C_2 symmetry, which are advantageous to Stark levels splitting of active ions and realization of new emission and tunable wavelength. Therefore, $RETaO_4$ can be used as new host matrices. Additionally, mixed crystal is an effective method to reduce lattice symmetry further and obtain the absorption and emission spectra with inhomogeneous broadening[9−10]. In the past decade, our group have finished a lot of research works on $RETaO_4$, especially on $GdTaO_4$ (GTO)[11]. On the base of the previous works, the GTO crystal field can be effectively regulated by mixing Y_2O_3. Moreover, the position of emission peaks can be regulated by the different-proportion of Y_2O_3 in $GdYTaO_4$ (GYTO) crystal. Now, rare earth(Ho, Nd)-doped GTO and GYTO have been realized laser output in near infrared band[12−15].

With the rapid development and application of laser technology, the search for new mid infrared laser materials has always been an important direction[16−20]. The $^5I_6 \rightarrow {}^5I_7$ transition of Ho^{3+} is an effective approach to obtain 2.9 μm lasers[21−22]. However, the laser efficiency is poor. Because of the long lifetime of $^5I_7$ level and the short lifetime of $^5I_6$, it is hard to realize population inversion, that is self-terminating "bottleneck" effect. To overcome this "bottleneck" effect, Pr^{3+} ions are usually used as deactivators to reduce the lifetime of low laser level, which have been achieved good results in other crystals[23−24]. In our previous work, the detailed properties of Ho-doped GYTO, Yb,Ho-doped GYTO, and Tm,Ho-doped GYTO are studied[25−27]. Unfortunately, there is no laser output. Therefore, Pr^{3+} ions are doped into Yb,Ho:GYTO to reduce the lifetime of the laser low level $^5I_7$.

In this study, a Yb,Ho,Pr:GYTO crystal was grown successfully using Czochralski method for the first time. The crystal structure and quality are analyzed. The polarized absorption spectra are investigated. The optical properties, including fluorescence, lifetimes, and energy transfer mechanisms among the ions are measured and analyzed.

1 Experimental details

1.1 Crystal growth

According to the chemical formula $Yb_{0.05}Ho_{0.01}Pr_{0.002}Gd_{0.738}Y_{0.2}TaO_4$, the high purity oxides were weighed, mixed, and calcined. The Yb,Ho,Pr:GYTO single crystal was grown by the Czochralski method. The temperature gradient, growth parameter, and growth process are the same as the previous work[26]. A transparent and crack free crystal with a size of Φ 23 mm × 40 mm was obtained, as shown in Fig.1(a). Under a 1 W 532 nm laser irradiation,

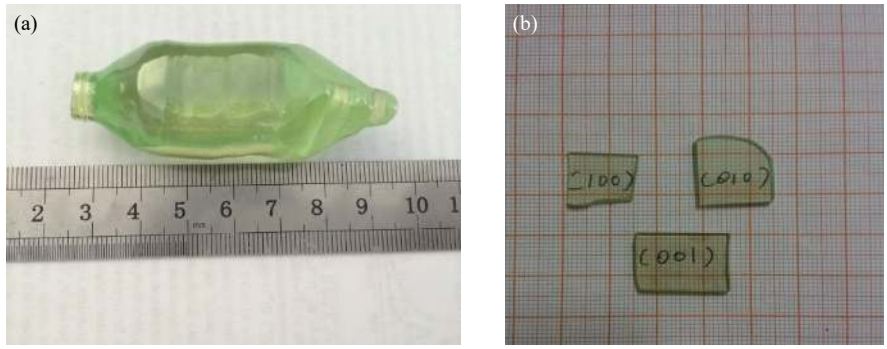

Fig.1 (a) Photograph of the as-grown Yb,Ho,Pr:GYTO crystal; (b) <100>, <010>, and <001>-oriented wafers of Yb,Ho,Pr:GYTO crystal

no light-scattering points were observed in the as-grown Yb,Ho,Pr:GYTO crystal. The <100>, <010>, and <001>-oriented slice samples were cut with a thickness of 2 mm and polished on both sides for measurements (shown in Fig.1(b)).

1.2 Characterizations

The X-ray diffraction (XRD) patterns of the as-grown Yb,Ho,Pr:GYTO crystal were measured using a Philip X′pert PRO X-ray diffractometer equipped with Cu Kα radiation. The diffraction peaks were recorded in the 2θ range of 10°-90° with a scan step of 0.033°. A high resolution X ′Pert Pro MPD diffractometer equipped with a hybrid Kα_1 monochromator was employed to collect the X-ray rocking curve. The doping concentrations of Yb^{3+}, Ho^{3+}, Pr^{3+} and Y^{3+} ions in the Yb,Ho,Pr:GYTO crystal were measured by Laser Ablation Inductively-Coupled Plasma Mass Spectrometry (LA-ICP-MS). The analyses of the sample which was cut from the shoulder part of the as-grown crystal were carried out on an Agilent 7900 quadrupole ICP-MS coupled to a Photon Machines equipped with Analyte HE 193 nm ArF Excimer Laser Ablation system. The effective segregation coefficients (k_{eff}) of the doping ions were obtained by comparing the LA-ICP-MS results with the initial concentrations in the raw materials used for crystal growth. Polarized absorption spectra were recorded at room temperature by using a Perkin-Elmer UV-VIS-NIR spectrometer (Lambda-900). In addition, we used a fluorescence spectrometer (Edinburgh FLSP920) with an exciting source of 940 nm LD and Opolette (OPO) 355I lasers to record the fluorescence spectrum from 2 850 to 3 000 nm and the fluorescence decay curves.

2 Results and discussion

2.1 Structure characterization, components analysis, and crystalline quality

The XRD patterns of the Yb,Ho,Pr:GYTO is shown in Fig.2. There are strong diffraction peaks,corresponding to (020), (110), (−121), (121), (040), (200), (002), (240), (042), (202), (−321), (−123), and (123) planes. The number and relative intensity of peaks are the same with the standard pattern of the GTO phase (ICSD-109186), which means that they belong to the same monoclinic space group of I2/a (No.15). Taking thestructure parameters of GTO as the initial values, the XRD data of Yb,Ho,Pr:GYTO crystal is fitted using the Rietveld refinement method to obtain the structural parameters. The refinement results of Yb,Ho,Pr:GYTO are shown in Fig.3 and Tab.1. The lattice parameters of Yb,Ho,Pr:GYTO are fitted to be a=5.381 Å(1Å=0.1 nm), b=11.023 Å, c=5.076 Å, β=95.59º, V=299.68 Å^3, which

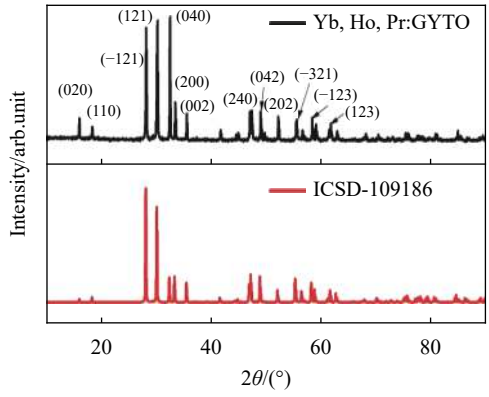

Fig.2 XRD patterns of Yb,Ho,Pr:GYTO single crystal

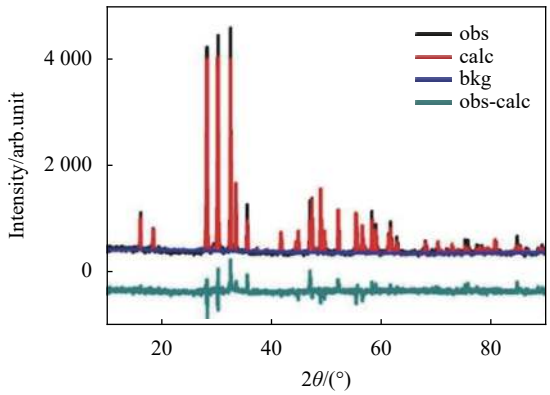

Fig.3 Rietveld refinement results from the XRD data of Yb,Ho,Pr:GYTO crystal

Tab.1 Structural parameters obtained by Rietveld refinement

Atom	*X*	*Y*	*Z*	Wyckoff site	U_{iso}
Gd	0.25	0.621 000	0.0	4*a*	0.025
Y	0.25	0.621 000	0.0	4*a*	0.025
Yb	0.25	0.621 000	0.0	4*a*	0.025
Ho	0.25	0.621 000	0.0	4*a*	0.025
Pr	0.25	0.621 000	0.0	4*a*	0.025
Ta	0.25	0.145 000	0.0	4*a*	0.025
O_1	0.094 000	0.460 000	0.254 000	8*c*	0.025
O_2	−0.007 00	0.717 000	0.293 000	8*c*	0.025

Cell parameters: a=5.381 Å, b=11.023 Å, c=5.076 Å, β=95.59°; Cell volume: V=299.68 Å^3; Space group: Monoclinic, I2/a (No.15); Density: ρ=8.630 g/cm^3; Reliability factors(R-factor): Rp=9.72%, R_{wp}=7.21%

are slightly smaller than the lattice parameters a=5.411, b=11.049, c=5.073, β=95.59º, V=302.56 Å^3 of GTO. The reason for this is that the sites of Gd^{3+} in GTO are occupied by Yb^{3+}, Ho^{3+}, Pr^{3+} and Y^{3+}, and their ionic radii are smaller than that of Gd^{3+}.

In recent years, inductively coupled plasma mass spectrometry (ICP-MS) is an effective detection for element concentrations measurement, especially trace element. However, the tested sample needs to be dissolved fully. Therefore, in this process, there are some shortcomings, such as insufficient dissolution, introduction of new impurities, which will lead to the incorrect results. The laser ablation inductively coupled plasma mass spectrometry (LA-ICP-MS) has become a preferred method for the measurement of major and trace element concentrations in mineral, gem, steel, ceramic, other synthetic and natural samples. It is a highly sensitive metal analytical technique and can realize microanalysis. Importantly, the tested sample does not need to be processed. In this study, a beam size of 15-40 μm and scan speeds of 15-40 μm/s (equal to beam size) were chosen. The repetition of 193 nm laser was 10 Hz with a constant energy output of 50 mJ, resulting in an energy density of 2-3 J/cm^2 at the target. Meanwhile, multi-point measurements of samples were carried out. Then the average value was calculated and the concentrations of doping ions Yb^{3+}, Ho^{3+}, Pr^{3+} and Y^{3+} ions in the as-grown crystal are shown in Tab.2. The k_{eff} of elements Yb, Ho, Pr, and Y are calculated according to the equation $k_{eff}=C_s/C_0$, where C_s and C_0 are the ion concentrations in the crystal and melt, respectively. The k_{eff} of Yb, Ho, Pr, and Y in Yb,Ho,Pr:GYTO crystal is 0.624, 1.220, 1.350, and 0.977, respectively.

Tab.2 Effective segregation coefficients (k_{eff}) of Yb, Ho, Pr, and Y in Yb,Ho,Pr:GYTO crystal

Element	Starting material (at %)	Crystal (at %)	k_{eff} (C_s/C_0)
Yb	0.05	0.031 2	0.624
Ho	0.01	0.012 2	1.220
Pr	0.002	0.002 7	1.350
Y	0.2	0.195 3	0.977

The X-ray rocking curves of the (100), (010), and (001) diffraction planes are shown in Fig.4. The three rocking curves are single diffraction peak with symmetric shape and without splitting, and the full widths at half maximum (FWHM) are 0.036°, 0.013°, and 0.077°,

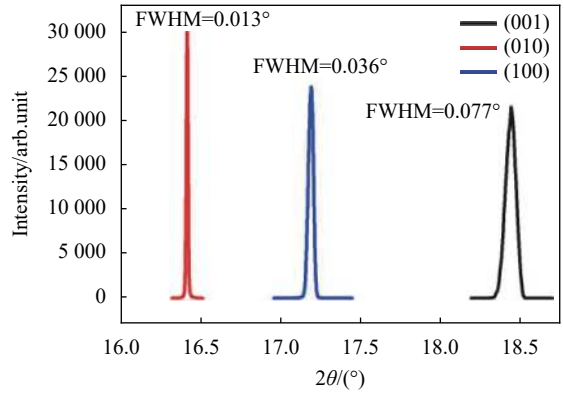

Fig.4 X-ray rocking curves of Yb,Ho,Pr:GYTO crystal

respectively. It indicates that the as-grown Yb, Ho, Pr:GYTO crystal is a single crystal with good crystalline quality.

2.2 Polarized absorption spectra

The room-temperature polarized absorption spectra of Yb,Ho,Pr:GYTO in the wavelength between 350 nm and 2 200 nm are shown in Fig.5(a). There are seven obvious absorption bands centered at around 360, 419, 450, 535, 645, 1 175, and 1945 nm, which correspond to the transitions starting from the $^5I_8$ ground state of Ho^{3+} to the excited states $^5G_5(1)+^3H_6$, $^5G_5$, $^5F_1+^5G_6$, $^5S_2+^5F_4$, $^5F_5$, $^5I_6$, and $^5I_7$ of Ho^{3+}, respectively. Importantly, the absorption bands from in the wavelength of 900-1 050 nm corresponds to the transition of Yb^{3+} ions from the ground state $^2F_{7/2}$ to the excited state $^2F_{5/2,}$ which matches well with the emission wavelength of commercially available high power InGaAs laser diodes (LD). For comparision, the 900-1 050 nm absorption bands of Yb,Ho:GYTO crystal and Yb,Ho,Pr:GYTO crystal are shown in Fig.5(b) and expressed in *a*, *b*, *c* and *a*', *b*', *c*' respectively. The absorption coefficient of E//*c* and E//*c*' are larger than those along the other directions of themselves.- Besides, the absorption coefficient of E//*c* is larger than that of E//*c*', which indicated that the crystal absorption coefficient was not influenced by Pr^{3+} doped in Yb,Ho,Pr:GYTO crystal. The dopant of Yb^{3+} ions in Yb,Ho,Pr:GYTO crystal was calculated to be 4.16×10^{20} cm^{-3}. Thus the absorption cross section of Yb,Ho,Pr:GYTO crystal can be calculated by the formula $\sigma_{abs}=\alpha(\lambda)/N$. Where σ_{abs} is the absorption cross section, $\alpha(\lambda)$ is the absorption coefficient, and N is the unit volume concentration of Yb^{3+} ions. The strongest absorption peaks are located at 958 nm, 932 nm, and 1 004 nm for E//*c*, corresponding to the absorption cross sections of 2.07×10^{-20} cm^2, 1.63×10^{-20} cm^2, and 1.03×10^{-20} cm^2. These strong absorption peaks are beneficial to improve pumping efficiency and reduce the dependence on the temperature of pump source.

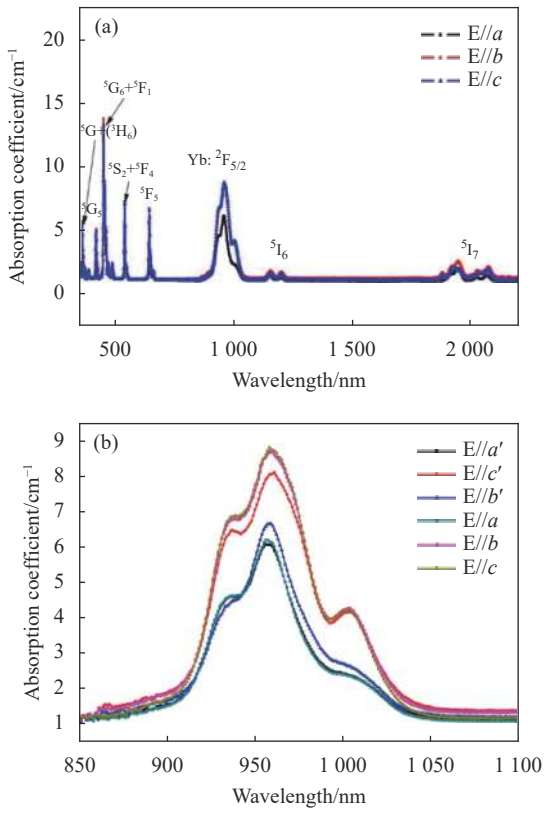

Fig.5 (a) Polarized absorption spectra of Yb,Ho,Pr:GYTO; (b) Comparization of Polarized absorption spectra of Yb,Ho,Pr:GYTO and Yb,Ho:GYTO in 850-1 100 nm (*a*, *b*, *c* →Yb,Ho,Pr:GYTO; *a*', *b*', *c*' →Yb,Ho:GYTO)

2.3 Luminescence properties

Figure 6 shows the emission spectrum of Yb,Ho,Pr: GYTO crystal in the wavelength range of 2 850-3 000 nm excited by 940 nm LD. In the 2.9 μm band, there is a strong emission peak, centered at 2 908 nm. The FWHM of 2 908 nm is about 15 nm. The wide emission peak is helpful to the tunability of laser wavelength. In addition, compared with that of Yb,Ho:GYTO crystal[27], the position of the strongest emission peak is shifted to the short wave direction by 2 nm, due to the little change of

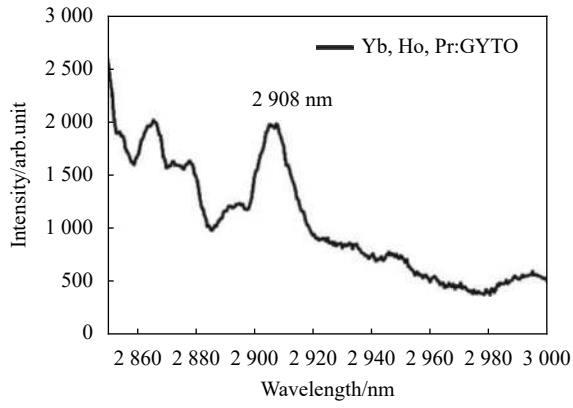

Fig.6 2.9 μm emission spectrum of Yb,Ho,Pr:GYTO crystal

crystal field with the doped of Pr^{3+}.

Furthermore, the stimulated emission cross section is calculated with the measured emission spectrum based on the Fchtbauer-Ladenburg equation:

$$\sigma_{em}=\frac{\beta\lambda^5 I(\lambda)}{8\pi n^2 c\tau_{rad}\int\lambda I(\lambda)\,d\lambda} \tag{1}$$

where $I(\lambda)$ is the emission intensity, λ is the emission wavelength, c is the speed of light, τ is the radiative lifetime of the upper energy level, and n is the refractive index, which is about 1.9[28]. The β factor is 16.324%, as reported in reference [25]. The maximum emission cross section at 2 908 nm is 1.44×10^{-19} cm^2. And the 2.9 μm emission cross section of Ho in GYTO and other hosts are presented in Tab.3. By comparison, the Yb,Ho, Pr:GYTO crystal possesses a larger emission cross section,- which suggests it is easier to realize laser output. However, the emission cross section of Yb,Ho,Pr:GYTO crystal is smaller than that of Yb,Ho:GYTO crystal, because of the deactivation of Pr^{3+} on the $^5I_6$ level. The details of the regulation of Pr^{3+} on energy level of Ho^{3+} are explained in the following part.

Tab.3 Comparison of the emission cross section for 2.9 μm in the different Ho^{3+} doped crystals

Crystals	Emission cross section (10^{-20} cm^2)
Yb,Ho,Pr:GYTO (this work)	14.4
Ho:GYTO[25]	12.6
Yb,Ho:GYTO[27]	18.9
Ho:LaF_3[29]	0.63
Ho:LuLF[30]	1.7
Ho:PbF_2[31]	1.44

The room temperature fluorescence decay curves of 1 204 nm ($^5I_6\rightarrow{}^5I_8$) and 2 068 nm ($^5I_7\rightarrow{}^5I_8$) emission of Yb,Ho,Pr:GYTO crystal excited by OPO pulse lasers are shown in Fig.7. Both of them are single exponential decay behavior. According to the fitted decay curves, the lifetimes of $^5I_6$ and $^5I_7$ level are 0.376 and 0.939 ms, respectively. Compared with the lifetimes of Yb,Ho:GYTO crystal as 0.419 and 7.298 ms, the Yb,Ho,Pr:GYTO crystal exhibits a remarkable attenuation of the $^5I_7$ level

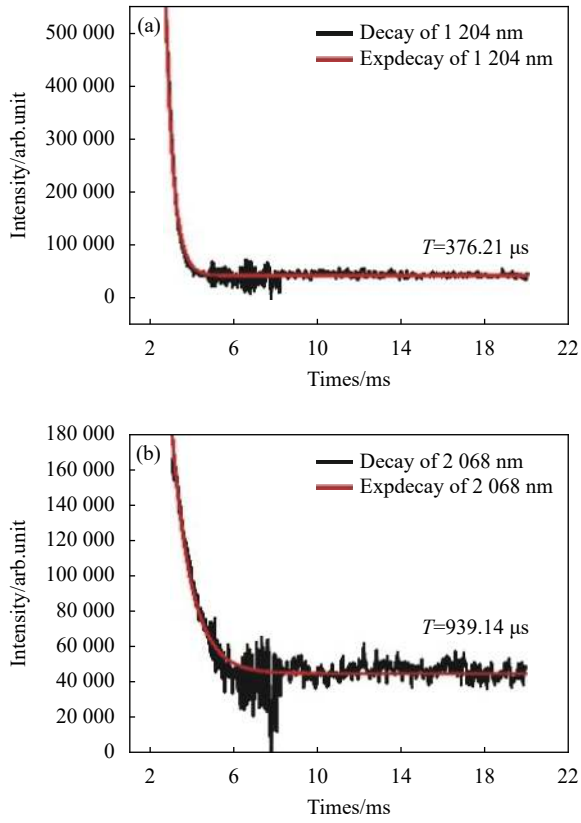

Fig.7 Fluorescence decay curves. (a) 1 204 nm ($^5I_6\rightarrow{}^5I_8$); (b) 2 068 nm ($^5I_7\rightarrow{}^5I_8$)

lifetime and little influence on the $^5I_6$ level. All these are attributed to the deactivation of Pr^{3+} through energy transfer between Ho-Pr in GYTO crystal. The energy transfer details are shown in Fig.8. The Yb^{3+} ions absorb pumping energy and transfer it to Ho^{3+} through cross-relaxation process. The emission from $^5I_6\rightarrow{}^5I_7$ of Ho^{3+} is located at 2.9 μm. Further doped with Pr^{3+}, the energy transfer (ET) between Ho^{3+} and Pr^{3+} are through two processes: ET_1, $^5I_6\rightarrow{}^3F_4+{}^3F_3$; ET_2, $^5I_7\rightarrow{}^3F_2+{}^3H_6$. The efficiency of energy transfer ET_1 and ET_2 is directly related to the lifetime of $^5I_6$ and $^5I_7$ levels. The higher the efficiency is, the more the level lifetime is reduced. In addition, the efficiency of energy transfer from the Ho^{3+} to Pr^{3+} ions can be calculated based on the following equation:

$$\eta=1-\frac{\tau_{DA}}{\tau_D} \tag{2}$$

where τ_{DA} is the level lifetime of Yb,Ho,Pr:GYTO with deactivated ion, and τ_D is the level lifetime of

Yb,Ho:GYTO without deactivated ion. According to equation (2) and the aforementioned level lifetimes of the Yb,Ho,Pr:GYTO and Yb,Ho:GYTO crystals, the energy transfer efficiencies of $Ho^{3+} \rightarrow Pr^{3+}$ in ET_1 and ET_2 processes are calculated to be about 10.26% and 87.13%, respectively. The energy transfer efficiency of ET_2 is greater than that of ET_1. Thus, the doping of Pr^{3+} ions can inhibit the self-termination phenomenon effectively. Population inversions between the $^5I_6$ and $^5I_7$ levels of the Ho^{3+} ions in Yb,Ho,Pr:GYTO crystal are likely to be realized at a lower pumping threshold.

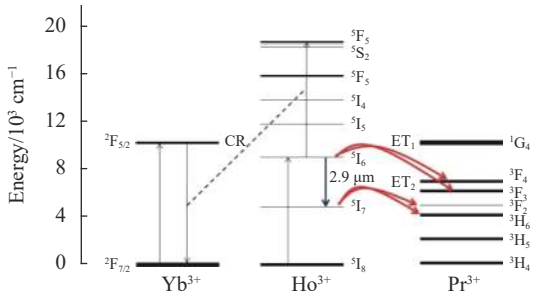

Fig.8 Schematic of energy transfer processes among Yb^{3+}, Ho^{3+}, and Pr^{3+} ions

Moreover, the upper and lower laser level lifetimes of other hosts are presented in Tab.4. From the table, we can see that the Yb,Ho,Pr:GYTO crystal possesses a shorter lifetime of the lower level $^5I_7$ and a similar lifetime of the upper level $^5I_6$, which are easier to realize-population inversion and laser output.

Tab.4 Comparison of the lifetimes of $^5I_7$ and $^5I_6$ in different crystals

Crystal	Ho ($^5I_7$)/ms	Ho ($^5I_6$)/ μs
Yb,Ho:YSGG[[32]]	10.2	585
Tm,Ho:YAG[[33]]	11.4	40
Yb,Ho,Pr:YAP[[24]]	1.258	341
Ho:GYTO[[25]]	8.081	311
Tm,Ho:GYTO[[26]]	4.09	131
Yb,Ho,Pr:GYTO (this work)	0.939	376

3 Conclusion

High-quality Yb,Ho,Pr:GYTO single crystal was successfully grown using Czochralski method. It belongs to the monoclinic space group of I2/a (No.15) and the lattice parameters are fitted to be a=5.381 Å, b=11.023 Å, c=5.076 Å, β=95.59°, V=299.68 Å^3. The k_{eff} of Yb, Ho, Pr, and Y in Yb,Ho,Pr:GYTO crystal are 0.624, 1.220, 1.350, and 0.977, respectively. The FWHM of X-ray rocking curves on the (100), (010), and (001) crystalline faces are 0.036°, 0.013°, and 0.077°, respectively, suggesting a high crystalline quality. The polarized absorption spectra indicate that the coefficient of E//c is larger than that of the other direction. The strongest absorption peaks are located at 958 nm, 932 nm, and 1 004 nm for E//c, corresponding to the absorption cross sections of 2.07×10^{-20} cm^2, 1.63×10^{-20} cm^2, and 1.03×10^{-20} cm^2. The strongest emission peak is located at 2 908 nm, and the FWHM is about 15 nm. Emission cross section at 2 908 nm is as large as 1.44×10^{-19} cm^2. Importantly, the lifetimes of $^5I_6$ and $^5I_7$ level are obtained to be 0.376 and 0.939 ms, 10.26% and 87.13% less than Yb,Ho:GYTO respectively. Therefore, the deactivator Pr^{3+} ions may be conducive to reducing the laser threshold and improving the conversion efficiency of the 2.9 μm laser in the Yb,Ho,Pr:GYTO crystal.

References:

[1] Liu W P, Zhang Q L, Zhou W L, et al. Growth and luminescence of M-Type and Tb: scintillation single crystals [J]. ***Nuclear Science IEEE Transactions on***, 2010, 57(3): 1287-1290.

[2] Yang H J, Zhang Q L, Zhou P Y, et al. Czochralski growth and optical investigations of Er^{3+}:$GdTaO_4$ laser crystal [J]. ***Proceedings of SPIE - The International Society for Optical Engineering***, 2012, 8206(1): 38.

[3] Siqueira K P F, Carmo A P, Bell M J V, et al. Optical properties of undoped $NdTaO_4$, $ErTaO_4$ and $YbTaO_4$ ceramics [J]. ***Journal of Luminescence***, 2016, 179: 146-153.

[4] Blasse G, Bril A. Luminescence phenomena in compounds with fergusonite structure [J]. ***Journal of Luminescence***, 1970, 3(2): 109-131.

[5] Voloshyna O, Neicheva S V, Starzhinskiy N G, et al. Luminescent and scintillation properties of orthotantalates with common formulae $RETaO_4$ (RE = Y, Sc, La, Lu and Gd) [J]. ***Materials Science & Engineering B***, 2013, 178(20): 1491-1496.

[6] Kazakova L I, Bykov I S, Dubovsky A B. The luminescence of rare-earth tantalate single crystals [J]. ***Journal of Luminescence***, 1997, 72–74: 211-212.

[7] Silva R A, Tirao G, Cusatis C, et al. Growth and structural characterization of M-type $GdTaO_4$ single crystal fiber [J]. ***Journal of Crystal Growth***, 2005, 274(3-4): 512-517.

[8] Brixner L. On the structural and luminescent properties of the M'LnTaO/sub$_4$/rare earth tantalates [J]. ***Chemischer Informationsdienst***, 1983, 130(12): 2435-2443.

[9] Peng F, Yang H J, Zhang Q L, et al. Growth, thermal properties, and LD-pumped 1066 nm laser performance of Nd^{3+} doped Gd/$YTaO_4$ mixed single crystal [J]. ***Optical Materials Express***, 2015, 5(11): 2536.

[10] Ding S J, Zhang Q L, Peng F, et al. Crysal growth, spectral properties, and continuous wave laser operation of Nd: $GdNbO_4$ [J]. ***Journal of Alloys and Compounds***, 2017, 693: 339-343.

[11] Dou R Q, Zhang Q L, Gao J Y, et al. Rare-earth tantalates and niobates single crystals: promising scintillators and laser materials [J]. ***Crystals***, 2018, 8(2): 55.

[12] Peng F, Yang H J, Zhang Q L, et al. Study on luminescence properties of Nd^{3+}-La^{3+} and Nd^{3+}-Sc^{3+} codoped M'-$LuTaO_4$ phosphors [J]. ***Optical Materials***, 2015, 39: 148-152.

[13] Peng F, Yang H J, Zhang Q L, et al. Spectroscopic properties and laser performance at 1,066nm of a new laser crystal Nd:$GdTaO_4$ [J]. ***Applied Physics B***, 2015, 118(4): 549-554.

[14] Duan X M, Chen G P, Qian C P, et al. Resonantly pumped high efficiency Ho:$GdTaO_4$ laser [J]. ***Optics Express***, 2019, 27(13): 18273-18281.

[15] Dai T Y, Guo S X, Duan X M, et al. High efficiency single-longitudinal-mode resonantly-pumped Ho:$GdTaO_4$ laser at 2068nm [J]. ***Optics Express***, 2019, 27(23): 34204-34210.

[16] Tempus M, Luthy W, Weber H P, et al. 2.79 μm YSGG:Cr:Er laser pumped at 790 nm [J]. ***IEEE Journal of Quantum Electronics***, 1994(11): 2608-2611.

[17] Högele A, Hörbe G, Lubatschowski H, et al. 2.70 μm CrEr: YSGG laser with high output energy and FTIR-Q-switch [J]. ***Optics Communications***, 1996, 125(1-3): 90-94.

[18] Guo H T, Liu L, Wang Y Q, et al. Host dependence of spectroscopic properties of Dy^{3+}-doped and Dy^{3+}, Tm^{3+}-codped Ge-Ga-S-CdI_2 chalcohalide glasses. [J]. ***Optics Express***, 2009, 17(17): 15350-15358.

[19] Faucher D, Bernier M, Androz G, et al. 20 W passively cooled single-mode all-fiber laser at 2.8 μm. [J]. ***Optics Letters***, 2011, 36(7): 1104-1106.

[20] Dickinson B C, Golding P S, Pollnau M, et.al. Investigation of a 791 nm pulsed-pumped 2.7 μm Er-doped ZBLAN fibre laser [J]. ***Optics Communications***, 2001, 191(3-6): 315-321.

[21] Diening A, Moebert P E A, Heumann E, et al. Diode-pumped cw lasing of Yb, Ho : KYF_4 in the 3μm spectral range in comparison to Er : KYF_4 [J]. ***Laser Physics***, 1998, 8(1): 214-217.

[22] Diening A, Kück S. Spectroscopy and diode-pumped laser oscillation of Yb^{3+}, Ho^{3+}-doped yttrium scandium gallium garnet [J]. ***Journal of Applied Physics***, 2000, 87(9): 4063-4068.

[23] Hudson D D, Williams R J, Withford M J, et al. Single-frequency fiber laser operating at 2.9 μm [J]. ***Optics Letters***, 2013, 38(14): 2388-2390.

[24] Zhang H L, Sun D L, Luo J Q, et al. Growth and spectroscopic investigations of Yb, Ho: YAP and Yb,Ho,Pr:YAP laser crystals [J]. ***Journal of Luminescence***, 2015, 158: 215-219.

[25] Dou R Q, Liu W P, Zhang Q L, et al. Growth and spectroscopic properties of Ho^{3+} doped $GdYTaO_4$ single crystal [J]. ***Journal of Luminescence***, 2018, 207: 213-219.

[26] Dou R Q, Zhang Q L, Liu W P, et al. Growth, structure, chemical etching, and spectroscopic properties of a 2.9 μm Tm,Ho:$GdYTaO_4$ laser crystal [J]. ***Optical Materials***, 2015, 48: 80-85.

[27] Dou R Q, Zhang Q L, Sun D L, et al. Growth, thermal, and spectroscopic properties of a 2.911 μm Yb,Ho:$GdYTaO_4$ laser crystal [J]. ***Crystengcomm***, 2014, 16(48): 11007.

[28] Wang X F, Liu W P, Sun H G, et al. Measurement of refractive indices of $GdTaO_4$ crystal by the auto-collimation method [J]. ***Acta Physica Sinica***, 2016, 65(8): 087801.

[29] Hong J, Zhang L, Zhang P, et al. Ho:LaF_3 single crystal as potential material for 2μm and 2.9μm lasers [J]. ***Infrared Physics & Technology***, 2016, 76: 636-640.

[30] Zhao C C, Hang Y, Zhang L H, et al. Polarized spectroscopic properties of Ho^{3+}-doped $LuLiF_4$ single crystal for 2 μm and 2.9 μm lasers [J]. ***Optical Materials***, 2011, 33(11): 1610-1615.

[31] Zhang P X, Yin J G, Zhang B T, et al. Intense 2.8 μm emission of Ho^{3+} doped PbF_2 single crystal [J]. ***Optics Letters***, 2014, 39(13): 3942-3945.

[32] Ch en, D W, Fincher C L, et al. Diode-pumped 1-W continuous-wave Er:YAG 3-μm laser [J]. ***Optics Letters***, 1999, 24(6): 385-387.

[33] Zhang H L, Sun D L, Luo J Q, et al. Growth and spectroscopic properties of the 2.9 μm Tm,Ho:LuAG laser crystal [J]. ***Optical Materials***, 2014, 34(4): 0416006.